Nanostructures

DOI: 10.1002/anie.201206940

A General Strategy for the Synthesis of Carbon Nanofibers from Solid Carbon Materials**

Yuxia Shen, Li Yan, Huaihe Song, Juan Yang, Gang Yang, Xiaohong Chen, Jisheng Zhou, Zhong-Zhen Yu, and Shubin Yang*

One-dimensional (1D) carbon nanotubes (CNTs) and nanofibers (CNFs) have attracted a lot of attention in recent years as a result of their unique structures and wide potential applications in biosensors,[1] gas storage, supercapacitors,[2] fillers in composites, nanofiltration membranes,[3] and gas chromatography columns.[4] Thus, extensive effort has been made to synthesize 1D carbon nanomaterials. In 1991, Iijima reported the synthesis of multiwalled carbon nanotubes, having unique structures, through arc evaporation[5] by using a graphite rod as the evaporation electrode; this report triggered great interest in CNTs all over the world. Subsequently, laser vaporization[6] of transition metal/graphite composite rods to produce CNTs was explored; this method is comparable to arc evaporation and has become one of the classical vapor-phase synthesis methods of CNTs. Meanwhile, chemical vapor deposition (CVD)[7] was also developed as a convenient and effective method for the large-scale synthesis of CNTs and CNFs. In the CVD process, most of the carbon sources are small molecular gases, such as CH_4 and C_2H_2. Very recently, solid-phase precursors have attracted intensive attention for the production of CNTs. In this regard, some organometallic compounds, such as iron phthalocyanine[8] and compounds containing butadiynyl ferrocene ,[9] and polymers, including ethyl borazines[10] and polypropylene,[11] were used to prepare CNTs. In essence, the pyrolysis of large molecules is also a CVD process, as the actual sources were small carbon species decomposed from the organometallic compounds. True solid-phase growth was first achieved by Harris et al.[12] They found that carbon nanotubes can be obtained at 3000 °C by direct pyrolysis of fullerene soot produced from arc evaporation, and pointed out that fullerene soot is an intermediate product. Chadderton and Chen[13] also discovered the presence of CNTs in the 1500 °C annealing product of milling graphite powder. Unfortunately, few CNTs were found and no clear mechanism was given for the growth of CNTs from solid carbon sources.[14]

Herein, we present a general strategy that uses solid carbon powders, such as artificial graphite (AG), activated carbon (AC), mesocarbon microbeads (MCMB), and acetylene black (AB), to grow many CNFs in the presence of metal catalysts. We found that the chemical oxidation of the carbon sources plays a key role in the formation of solid-phase carbon fragments. In addition, the molten catalyst is also necessary to grow CNFs as it can supply sufficient contact with solid-phase carbon fragments. This inexpensive general strategy is expected to trigger a revolution in nanocarbon preparation, for which small molecular carbon sources (such as carbon gases and laser sputtered graphite electrodes) traditionally play a leading role. Most importantly, this general method provides insight into the mechanism for the formation of CNFs from solid precursors, thus giving us a novel perspective on the formation of one-dimensional carbon nanomaterials.

Initially, we used AB as the solid precursor, and CNFs could be formed at a carbonization temperature of 1500 °C (Figure 1). The CNFs where scattered around Fe@C spheres and exhibited cobweb-like morphology (Figure 1 a). The C/Fe element ratio is 1.63 for these eutectic spheres and was measured by energy dispersive X-ray spectroscopy (EDS, EDAX GENESIS 60; see the Supporting Information, Figure S1). Notably, the CNFs directly grow out from these spheres (Figure 1 b). Most interestingly, the CNFs possess varied diameters that are larger at the root close to the sphere than for other parts of the CNFs, thus implying that the changing carbon atom concentration plays the major role in the formation of CNFs. This character can be found in most of the CNFs obtained by this method, and in some cases coalescence of the ends of the CNFs is seen (see the Supporting Information, Figure S2), thus suggesting that the growth of CNFs here may involve some kind of melting process. Apart from at the roots, the CNFs show the average diameter of 50 nm and length of about 10 μm with an aspect ratio of about 200 (Figure 1 c). The objects adhered to the CNFs and spheres are the residual carbon sources. When washed with dilute hydrochloric acid, the spheres would be damaged or disappear, to leave pure carbon materials (Figure 1 d). The characteristic XRD peaks of CNFs are displayed in Figure S3 (see the Supporting Information). There is one sharp reflection around $2\theta = 26°$ and three weak and broad reflections at 43°, 53°, and 80°, corresponding to the

[*] Y. Shen, L. Yan, Prof. H. Song, J. Yang, G. Yang, Prof. X. Chen, Dr. J. Zhou, Prof. Z.-Z. Yu
State Key Laboratory of Chemical Resource Engineering
Key Laboratory of Carbon Fiber and Functional Polymers
Ministry of Education, Beijing University of Chemical Technology
Beijing 100029 (P.R. China)
E-mail: songhh@mail.buct.edu.cn
Dr. S. Yang
Department of Mechanical Engineering and Materials Science
Rice University, 6100 Main Street, Houston, TX 77006 (USA)

[**] This work was supported by the National Natural Science Foundation of China (50572003 and 50972004), the State Key Basic Research Program of China (2006CB9326022006), and the Foundation of Excellent Doctoral Dissertation of Beijing City (YB20081001001).

Supporting information for this article is available on the WWW under http://dx.doi.org/10.1002/anie.201206940.

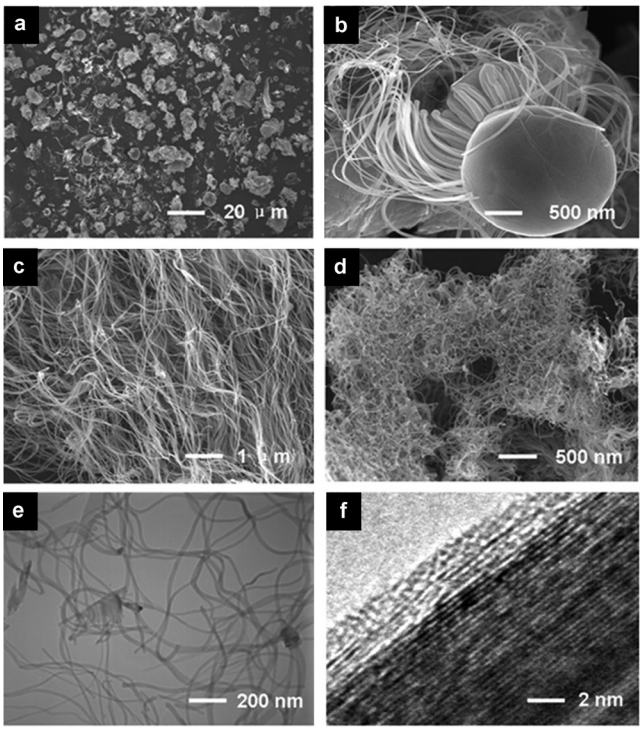

Figure 1. Morphologies and structures of CNFs grown from AB by using Fe as catalyst at 1500 °C. a–d) SEM images of CNFs, e) TEM image of CNFs, and f) HRTEM image of a typical single CNF. Resolution: 300 dpi.

diffraction peaks of the (002), (100), (004), and (110) lattice planes of carbon, respectively.[15]

TEM image of the product shows winding CNFs (Figure 1 e). To obtain detailed information about the structure of an individual CNF an HRTEM image was obtained (Figure 1 f). The CNFs have an obvious core-shell structure. The outside rough graphene layers have a thickness of around 5 nm and exhibit a relatively disordered carbon structure, which may be generated from the deposition of amorphous carbon, whereas the regular (002) lattice fringes in internal layers are remarkably straight and parallel to the fiber axis; these internal layers would be formed from the catalytic reaction of the solid carbon source with the catalyst. This core-shell carbon architecture has also been observed by Endo et al in vapor-grown carbon fibers.[16]

As well as AB, we also found that other solid carbon sources such as AG, AC, and MCMB can also be used to prepare CNFs by the same process, thus implying that this is a general approach for the preparation of carbon nanofibers. SEM images revealed that the CNFs obtained from different carbon sources present similar morphologies (Figure 2), and these CNFs are designated as CNFs-AG, CNFs-AC, and CNFs-MCMB according to their carbon precursor. CNFs with diameters of 40-80 nm were successfully obtained from all the different carbon sources. The fact that a wide range of solid carbon sources can be used for the formation of CNFs implies that the exfoliation of nano-sized graphitic fragments with many oxygen functionalities and/or dangling bonds is feasible. These fragments are considered as the real carbon source that participates in the growth of CNFs.

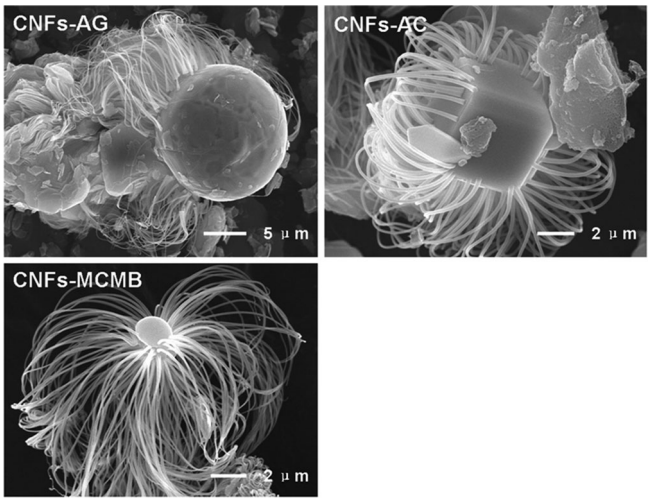

Figure 2. SEM images of CNFs grown from oxidized AG, AC, and MCMB by using Fe as catalyst at 1500 °C. Resolution: 300 dpi.

It is worth pointing out that the crystallinity of the obtained CNFs is directly dependent upon their carbon precursors. This correlation was revealed by Raman spectra of AB, AG, and the CNFs obtained from these sources (see the Supporting Information, Figure S4). Detailed data and calculations are shown in Table S1 (see the Supporting Information). The full width at half maximum (FWHM-G) is associated with hexagonal crystals consisting of sp^2-hybridized carbon atoms. As the FWHM-G value for AB is higher than that for AG, the higher FWHM-G for CNFs-AB compared to that of CNFs-AG is reasonable. The intensity ratio of the D band and G band (I_D/I_G) has been generally used to quantify the density of defects in materials containing sp^2-hybridized carbon atoms.[17] Although undergoing the same oxidation process, AB has a much larger density of defects than AG. Correspondingly, the density of defects in the CNFs-AB is also relatively larger. Notably, although a solid carbon source with a high degree of graphitization is expected to give CNFs with enhanced crystallinity, the high structure regularity of the carbon source is a disadvantage for the exfoliation of carbon fragments and thus adversely affects the yield of CNFs. Therefore a carbon source with poor structure regularity always leads to a more successful growth of CNFs. However, CNTs with high structure regularity are usually necessary for mechanical applications, and therefore it is important to find a balance between the exfoliation ability of solid carbon sources and the crystallinity of the CNFs.

Chemical oxidation by using an mixture of acids introduces considerable oxygen-containing functional groups onto the graphene layers, and even breaks the skeleton C=C bonds, thus leaving carbon fragments with dangling bonds on the edges. Generally, dangling bonds or lattice defects on graphitic layers may promote the formation of curved structures,[18] which is required for CNT formation. Buchholz[19] et al. have described in detail the roles of the structural defects in the growth of CNTs. The introduction of curvature driven by the insertion of pentagon and heptagon rings, and pentagon–heptagon pairs into a hexagonal network is a key element for the growth of CNTs. The presence of these defects were

confirmed by the XRD patterns of AB at a different oxidation time (see the Supporting Information, Figure S5). The fact that carbon particles rather than CNFs were obtained when using untreated AB also confirms the importance of activation during the growth of CNFs. The use of oxidized AB as carbon sources always leads to an increased probability of formation and yield of CNFs.

The growth temperature is considered as a critical factor in the CVD method. Lee et al.[20] pointed out that the growth temperature could control the growth rate, diameter, density, and crystallinity of CNTs. Recently, Takagi et al. realized that molten metal catalysts are favorable for the formation of CNTs in CVD.[21] Kataura et al.[22] emphasized that CNTs start to grow just when the temperature is close to the eutectic temperature of the metal catalyst. In our system, to facilitate the contact of the metal catalyst with the solid carbon sources and form the metal eutectic system, the temperature at which the metal fuses is critically important. Taking Fe for example, the liquid or liquid-like phase is expected at 1500 °C, as the melting point of bulk Fe is 1535 °C and a lower melting point is expected for nanoparticles.[23] The considerable number of syntheses that failed when they were conducted at 1300 °C and 1400 °C (or at even lower temperatures) confirms the importance of the melting process.

The short reaction time and the required high temperatures involved in CNT evolution usually make it difficult to investigate the evolution mechanism. Herein, we successfully observed the detailed morphologies and structures of the obtained intermediates and various products related to CNFs. In the transformation of solid-phase carbon sources into CNFs the evolution of Fe eutectic spheres (Figure 3a) and their transformation into CNFs was revealed: scattered "buds" burst out of micrometer-sized eutectic spheres at suitable temperatures and when there is a sufficient carbon content, some of these buds gradually grow thinner and longer, thus forming intermediates to CNFs (Figure 3b). These elongated buds grow into CNFs and more buds are formed, until the local carbon species are consumed. Concentrated areas of winding CNFs encapsulate residual Fe eutectic spheres (Figure 3c). Notably, these structures bifurcate and the branched locations gradually become thinner and thinner, leaving "garlic clove" or "comb-like" morphologies. These morphologies always share the same intermediates, and parts of the CNFs clusters coalesce (Figure 3c and d). With adequate time at optimal temperature, large amounts of CNFs with diameters of 50–80 nm can be obtained (Figure 3d).

The observation that CNFs can be produced from solid carbon sources prompted us to investigate the transformation of 3D to 1D carbon materials (Figure 4). For the growth mechanism of CNTs or CNFs prepared through previous methods, the fragments were usually gases, liquids, or sputtered carbon atoms. However, as the furnace temperatures ($\leq$1500 °C) used in this system are far below the melting point of carbon (3527 °C)[14] and the carbonization was carried out at a slower heating rate (5 °C min^{-1}) rather than by instantaneous heating to high temperatures, the fragments are still in the solid state and the growth of CNFs involves a totally solid-phase transformation. The molten

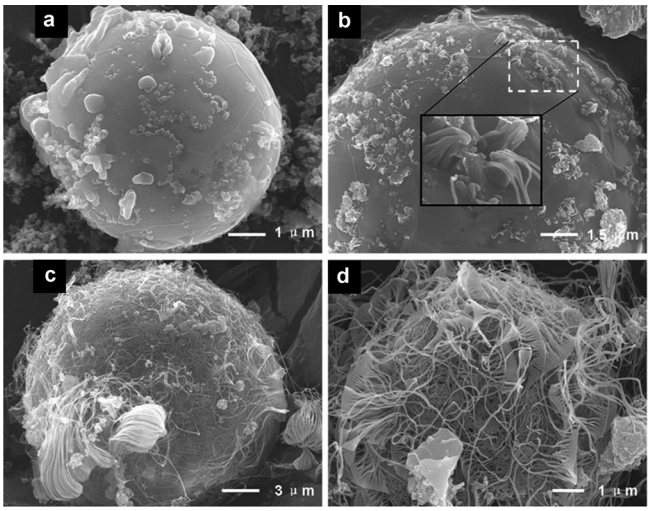

Figure 3. Intermediates in the growth of CNFs. The evolution from dumpy buds to fine filaments on the surfaces of spheres, after carbon fragments have precipitated from Fe solutions is shown. Resolution: 300 dpi.

metal catalysts have sufficient contact with highly oxidized fragments and further coalesce into Fe@C eutectic spheres, thus minimizing the surface energy. Therefore the Fe@C eutectic spheres would be considered as the intermediates in the growth of CNFs. These carbon and metal mixtures have also been demonstrated and simulated by Shibuta and Maruyama,[24] and their formation is considered characteristic in the growth of CNFs from bulk carbon sources. The carbon species stripped from solid-phase carbon sources, such as common carbon sources, adsorbed, diffused, and precipitated throughout the molten metals. Unlike previous methods, the process happens within these eutectic micrometer spheres, as

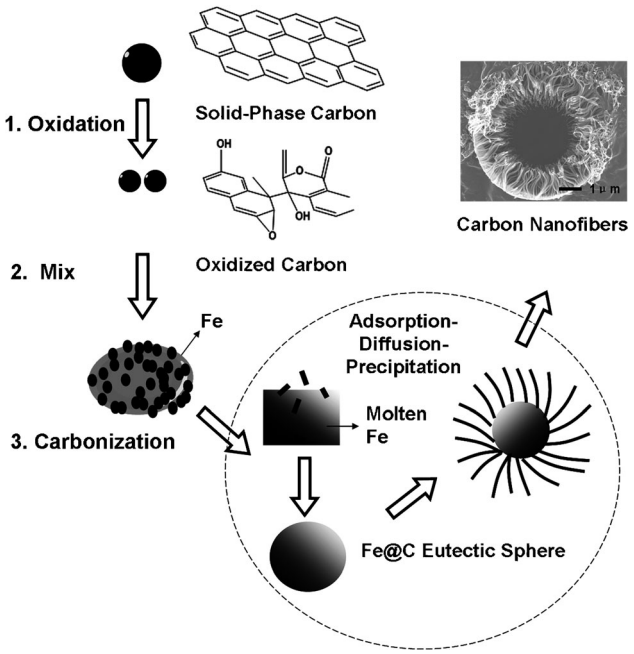

Figure 4. Illustration of the growth of CNFs from solid-phase carbon. Resolution: 1000 dpi.

mentioned above. As the concentration of dissolved carbon in the metal increases a supersaturated solution is formed, thus promoting the precipitation of carbon fragments onto the surface of the metal, accompanied by formation of curved graphene layers; structural defects to these curved graphene layers caused by the carbon fragments play an important role in CNF formation. In the precipitation process, metal particles would be pushed to the tips of the CNFs driven by the pressure buildup, as summarized by Krijn et al.[25] We hypothesize that the process is terminated as a result of changes in the local temperature or complete consumption of the carbon fragments.

A simple and efficient strategy was developed to prepare CNFs from general solid carbon sources. The chemical oxidation of carbon sources plays a key role in the formation of oxidized solid-phase carbon fragments. The molten metal catalyst is also necessary to achieve sufficient contact with solid-phase carbon fragments. The general adaptability of this process offers us improved understanding about the control of carbon nanostructures and the effective utilization of abundant solid carbon sources, including the carbon and graphite waste.

Experimental Section

Materials: The following carbon materials were chosen as the carbon sources to synthesize CNFs: artificial graphite (AG, average size: 10–20 μm), activated carbon (AC, specific surface area $>1800\ m^2 g^{-1}$, carbon content $\geq 95\%$), mesocarbon microbeads (MCMB, carbon content $\geq 94\% \approx 95\%$, average size: 20 μm), and acetylene black (AB, average size: 30 nm, carbon content $\geq 99\%$).

Preparation of CNFs: The whole process is illustrated in Figure 5 and includes three steps: 1) Oxidation. The solid carbon source (0.5 g) was oxidized by H_2SO_4 (98%)/HNO_3 (70%) (3:1, volume ratio; 12 mL) at 80 °C for 40 to 100 h and then was washed with deionized water until the pH value reached neutral. 2) Mix. The oxidized carbon material was added to a solution of $FeCl_3{\cdot}6H_2O$ (0.7 g) in ethanol (25 mL). The mixture was stirred at room temperature to obtain a mixture of carbon and catalyst precursor. 3) Carbonization. The mixture of carbon and catalyst was heated under argon and maintained at 1500 °C for several hours. After the furnace was allowed to cool to room temperature, the final CNFs were obtained. To remove residual metal catalyst, the carbonized products were washed with dilute hydrochloric acid (24%; 55 mL).

Characterization: The products were characterized by transmission electron microscope (TEM, H-800), High-resolution transmission electron microscope (HRTEM, JEOL JEM-2010), field-emission scanning electron microscope (FE-SEM, Hitachi S-4700), and X-ray diffraction (XRD, D/max 2400X) using Cu Kα radiation ($\lambda = 1.5406$ Å). Raman spectra were acquired on a Renishaw *inVia* Raman microscope using an excitation wavelength of 514.5 nm, the experiments were performed under ambient conditions.

Received: August 28, 2012
Published online: October 29, 2012

Keywords: carbon nanofibers · nanostructures · oxidation · reaction mechanisms · solid carbon materials

[1] P. W. Barone, S. Baik, D. A. Heller, M. S. Strano, *Nat. Mater.* **2005**, *4*, 86–92.
[2] C. Niu, E. K. Sichel, R. Hoch, D. Moy, H. Tennent, *Appl. Phys. Lett.* **1997**, *70*, 1480–1482.
[3] a) J. K. Holt, H. G. Park, Y. M. Wang, M. Stadermann, A. B. Artyukhin, C. P. Grigoropoulos, A. Noy, O. Bakajin, *Science* **2006**, *312*, 1034–1037; b) B. J. Hinds, N. Chopra, T. Rantell, R. Andrews, V. Gavalas, L. G. Bachas, *Science* **2004**, *303*, 62–65.
[4] C. Saridara, S. Mitra, *Anal. Chem.* **2005**, *77*, 7094–7097.
[5] S. Iijima, *Nature* **1991**, *354*, 56–58.
[6] T. Guo, P. Nikolaev, A. Thess, D. T. Colbert, R. E. Smalley, *Chem. Phys. Lett.* **1995**, *243*, 49–54.
[7] a) S. Iijima, T. Ichlhashi, *Nature* **1993**, *363*, 603–605; b) R. Andrews, D. Jacques, A. M. Rao, F. Derbyshire, D. Qian, X. Fan, E. C. Dickey, J. Chen, *Chem. Phys. Lett.* **1999**, *303*, 467–474.
[8] L. Zhi, T. Gorelik, R. Friedlein, J. Wu, U. Kolb, W. R. Salaneck, K. Müllen, *Small* **2005**, *1*, 798–801.
[9] M. Laskoski, T. M. Keller, S. B. Qadri, *Carbon* **2007**, *45*, 443–448.
[10] R. Brydson, A. V. K. Westwood, X. Jiang, S. J. Rowen, S. Collins, S. Lu, B. Rand, K. Wade, R. Coult, *Carbon* **1998**, *36*, 1139–1147.
[11] U. Arena, M. L. Mastellone, G. Camino, E. Boccaleri, *Polym. Degrad. Stab.* **2006**, *91*, 763–768.
[12] P. J. F. Harris, S. C. Tsang, J. B. Claridge, M. L. H. Green, *J. Chem. Soc. Faraday Trans.* **1994**, *90*, 2799–2802.
[13] L. T. Chadderton, Y. Chen, *Phys. Lett. A* **1999**, *263*, 401–405.
[14] P. J. F. Harris, *Carbon* **2007**, *45*, 229–239.
[15] L. Dobiášová, V. Starý, P. Glogar, V. Valvoda, *Carbon* **1999**, *37*, 421–425.
[16] M. Endo, Y. A. Kim, T. Hayashi, K. Nishimura, T. Matusita, K. Miyashita, M. S. Dresselhaus, *Carbon* **2001**, *39*, 1287–1297.
[17] A. Jorio, M. M. Lucchese, F. Stavale, E. H. M. Ferreira, C. Vilani, M. V. O. Moutinho, R. B. Capaz, C. A. Achete, *Carbon* **2010**, *48*, 1592–1597.
[18] J. Y. Huang, H. Yasuda, H. Mori, *Chem. Phys. Lett.* **1999**, *303*, 130–134.
[19] D. B. Buchholz, S. P. Doherty, R. P. H. Chang, *Carbon* **2003**, *41*, 1625–1634.
[20] C. J. Lee, J. Park, Y. Huh, J. Y. Lee, *Chem. Phys. Lett.* **2001**, *343*, 33–38.
[21] D. Takagi, H. Hibino, S. Suzuki, Y. Kobayashi, Y. Homma, *Nano Lett.* **2007**, *7*, 2272–2275.
[22] H. Kataura, Y. Kumazawa, Y. Maniwa, Y. Ohtsuka, R. Sen, S. Suzuki, Y. Achiba, *Carbon* **2000**, *38*, 1691–1697.
[23] A. Moisala, A. G. Nasibulin, E. I. Kauppinen, *J. Phys. Condens. Matter* **2003**, *15*, S3011–S3035.
[24] Y. Shibuta, S. Maruyama, *Chem. Phys. Lett.* **2003**, *382*, 381–386.
[25] P. Krijn, D. Jong, J. W. Geus, *Catal. Rev.* **2000**, *42*, 481–510.

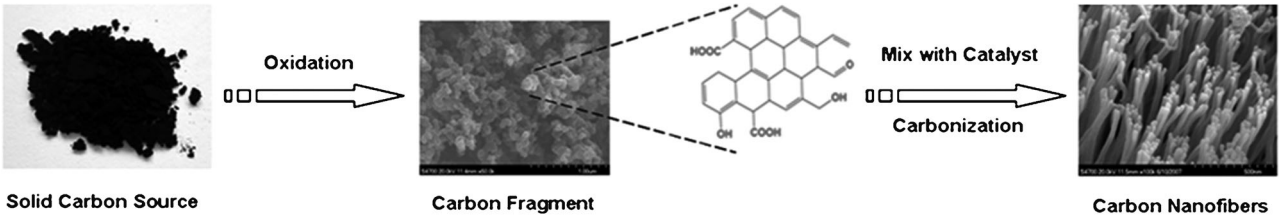

Figure 5. Schematic illustration of the procedure for the growth of CNFs from a solid carbon source. Resolution: 1000 dpi.

